

AIAA 82-4008

Kelvin-Helmholtz Stability Analysis of Air Cushion Landing Gear Trunk Flutter

Michael Hinchey* and Philip Sullivan†

Institute for Aerospace Studies, University of Toronto,
Ontario, Canada

Introduction

A PROBLEM which has been encountered during the development of bag or trunk-type air cushion landing gear is trunk flutter. A recent review of experimental data on this phenomenon obtained from a modified de Havilland Buffalo known as the XC-8A and a test apparatus is given by Boghani and Fish.¹ It was observed that flutter occurs most often at the bottom of the trunk, where the air gap is a minimum, as shown in Fig. 1. From the results of their own experimental and theoretical work they concluded that flutter occurs when the negative stiffness associated with the airflow under the trunk becomes, in an absolute value sense, greater than the positive stiffness associated primarily with trunk tension. In other words, they suggested that flutter arises from a static instability, and that the oscillations occur as a result of the nonlinear aspects of the problem. However, they presented an analysis of the dynamics of the phenomenon, in which the trunk was modeled as a series of discrete masses connected by springs. The latter simulated the tensile stiffness of the trunk. The airflow between the trunk and the ground was considered to be one-dimensional, inviscid, incompressible, and quasisteady. Also this flow was assumed to separate from the trunk downstream of the minimum air gap at that point for which the trunk is inclined at an angle $\theta = 12$ deg with respect to the ground plane, as shown in Fig. 1. This angle was obtained from a separate steady-state experiment.

The purpose of this Note is to show that a Kelvin-Helmholtz type linear stability analysis,^{2,3} similar to those used for aeroelastic problems such as panel flutter, predicts a divergent oscillation at about the conditions for which flutter was observed. Hence the flutter is not necessarily the result of a static instability, as is suggested in Ref. 1.

Kelvin-Helmholtz Analysis

The simplified geometry used for the analysis is shown in Fig. 2. The trunk is modeled locally as a membrane of infinite extent set parallel to the ground plane. There is no variation in the mean or steady-state properties with respect to the streamwise coordinate x ; and the ground plane is located at $y = -h$ directly below the membrane. The airflow beneath the membrane, and any that is induced above it, is assumed to be two-dimensional, incompressible, unsteady, and irrotational. This implies that the flows are governed by Laplace's equation:

$$\nabla^2 \phi = \frac{\partial^2 \phi}{\partial x^2} + \frac{\partial^2 \phi}{\partial y^2} = 0 \quad (1)$$

Let U be the mean flow velocity under the trunk, p the static pressure, ρ_a the air density, g the gravitational acceleration, and η the vertical displacement of the membrane. Using the superscripts b and t to denote the flow beneath the trunk and directly above it respectively, one can write the boundary conditions imposed on the flows by the trunk motion as

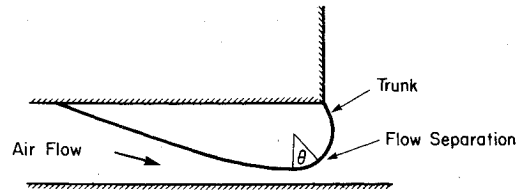


Fig. 1 Trunk geometry.

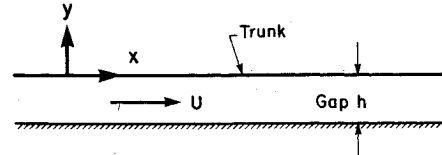


Fig. 2 Kelvin-Helmholtz geometry.

follows:

- 1) Unsteady Bernoulli conditions, at $y = 0$,

$$\text{bottom: } \frac{\partial \phi^b}{\partial t} + U \frac{\partial \phi^b}{\partial x} + \frac{p^b}{\rho_a} + g\eta = 0 \quad (2)$$

$$\text{top: } \frac{\partial \phi^t}{\partial t} + \frac{p^t}{\rho_a} + g\eta = 0 \quad (3)$$

- 2) Kinematic conditions, at $y = 0$,

$$\text{bottom: } \frac{\partial \eta}{\partial t} + U \frac{\partial \eta}{\partial x} = \frac{\partial \phi^b}{\partial y} \quad (4)$$

$$\text{top: } \frac{\partial \eta}{\partial t} = \frac{\partial \phi^t}{\partial y} \quad (5)$$

The equation governing the trunk motion is

$$\rho_m \frac{\partial^2 \eta}{\partial t^2} = p^b - p^t + T \frac{\partial^2 \eta}{\partial x^2} - K_s \eta \quad (6)$$

where ρ_m is the surface density of the membrane, T is the membrane tension, and K_s is the local stiffness. At the ground ($y = -h$) and at $y = +\infty$,

$$\frac{\partial \phi}{\partial y} = 0 \quad (7)$$

Consider a wave traveling in the positive x direction described by

$$\eta = \eta_0 e^{i(kx - \omega t)} \quad (8)$$

$$\phi^b = \phi_0^b \cosh[k(h + y)] e^{i(kx - \omega t)} \quad (9)$$

$$\phi^t = \phi_0^t e^{-ky} e^{i(kx - \omega t)} \quad (10)$$

where ω is the wave angular frequency, k is the wave number, and η_0 , ϕ_0^b , and ϕ_0^t are wave amplitudes. Substitution of Eqs. (9) and (10) into Eq. (1) shows that these forms automatically satisfy Laplace's equation. Substitution also shows that Eq. (7) is satisfied. The membrane condition yields

$$p^b - p^t = -\rho_m \omega^2 \eta + Tk^2 \eta + K_s \eta \quad (11)$$

Substitution of this expression into the unsteady Bernoulli conditions gives, after some manipulation,

$$\begin{aligned} & -i\omega \phi_0^b \cosh[kh] + Uik\phi_0^b \cosh[kh] \\ & - \frac{\rho_m}{\rho_a} \omega^2 \eta_0 + \left(\frac{Tk^2 + K_s}{\rho_a} \right) \eta_0 + i\omega \phi_0^t = 0 \end{aligned} \quad (12)$$

Received Aug. 19, 1981. Copyright © American Institute of Aeronautics and Astronautics, Inc., 1981. All rights reserved.

*Research Associate, Air Cushion Vehicle Group.

†Associate Professor, Head of Air Cushion Vehicle Group.

Table 1 XC-8A data

Gap	$h = 2.13 \text{ cm}$	0.07 ft
Density ratio	$\rho_a / \rho_m = 0.088 \text{ m}^{-1}$	$\rho_a = \text{standard atmospheric density}$
Stiffness	$K_s^a = 4.71 \times 10^5 \text{ N/m}^3$	3000 lb/ft ³
Tension	$T^b = 1.31 \times 10^4 \text{ N/m}$	900 lb/ft

^a Rough estimate: $K_s = \Delta p_{\text{suction}} / \Delta h$. ^b Rough estimate: $T = \text{bag radius} \times \text{bag pressure}$.

The kinematic conditions reduce to

$$-i\omega\eta_0 + Uik\eta_0 = k \sinh[kh] \phi_0^b \quad (13)$$

$$-i\omega\phi_0 = -k\phi_0^b \quad (14)$$

Solving Eqs. (13) and (14) for ϕ_0^b and ϕ_0^i in terms of η_0 and substituting into Eq. (12) yields the following characteristic equation for the frequency

$$A\omega^2 + B\omega + C = 0 \quad (15)$$

where

$$A = 1 + \left(\frac{\rho_m}{\rho_a} + \frac{1}{k} \right) k \tanh[kh]$$

$$B = -2Uk \quad (16)$$

$$C = - \left(\frac{Tk^2 + K_s}{\rho_a} \right) k \tanh[kh] + U^2 k^2$$

Solving the quadratic for ω yields the dispersion relationship

$$\omega = \frac{-B \pm \sqrt{B^2 - 4AC}}{2A} \quad (17)$$

If $B^2 - 4AC$ is less than zero, a complex conjugate pair of roots results.

Equation (8) shows that the root with the positive imaginary part will be unstable. Hence the condition $B^2 - 4AC = 0$ represents a stability boundary. It yields the following equation for critical flow velocity U_c as a function of wave number k :

$$U_c = k^{-1} \left\{ \left(\frac{Tk^2 + K_s}{\rho_a} \right) \left(\frac{\rho_a k}{\rho_m k + \rho_a} + k \tanh[kh] \right) \right\}^{1/2} \quad (18)$$

By plotting U_c as a function of k one finds that the curve has a minimum at some value $k = k_c$. This minimum identifies the wave number associated with the onset of flutter. The corresponding flutter frequency is given by

$$\omega = \frac{-B}{2A} = U_c k_c \left\{ 1 + \left(\frac{\rho_m}{\rho_a} + \frac{1}{k_c} \right) k_c \tanh[k_c h] \right\}^{-1} \quad (19)$$

Results and Discussion

A suction pressure occurs at the minimum gap because the flow does not separate there. In Ref. 1 this suction pressure was measured to be approximately 1.75 times the cushion pressure below atmospheric. Thus

$$U_{\text{gap}} \approx \sqrt{\frac{2(p_c + 1.75p_c)}{\rho_a}} \quad (20)$$

Two cushion pressures were considered in Ref. 1 for the XC-8A. For the lower pressure (3.8 kPa) no flutter occurred, and U_{gap} according to Eq. (20) was 133 m/s. For the higher pressure (6.2 kPa), flutter did occur and U_{gap} according to Eq. (20) was 169 m/s. The data in Ref. 1 were used here to estimate the various coefficients in Eq. (18) (see Table 1), and the plot of U_c vs k given in Fig. 3 was obtained. This gives a

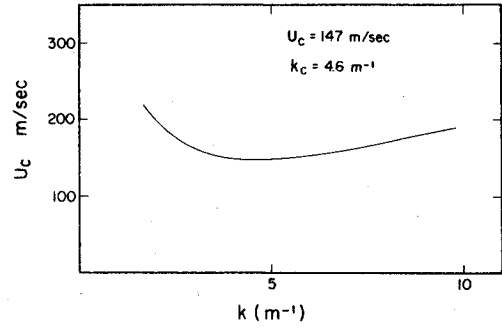


Fig. 3 Critical flow velocity vs wave number.

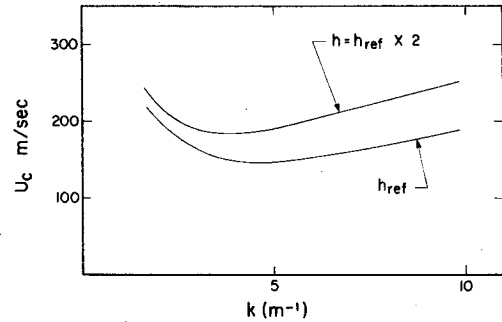


Fig. 4 Gap effect.

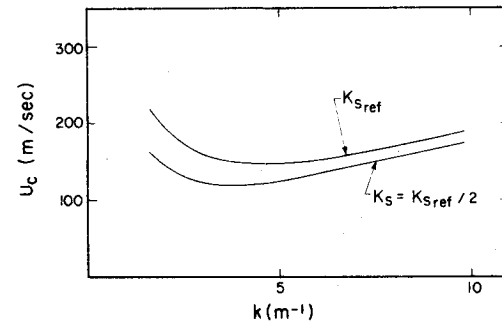


Fig. 5 Stiffness effect.

minimum value of $U_c = U_{cm} = 147 \text{ m/s}$, which is bracketed by the two values noted above. The frequency f_c obtained in Ref. 1 was 28 Hz. The present analysis gives 40 Hz. The negative stiffness-positive stiffness argument gives

$$U_c = \sqrt{K_s h / \rho_a} \quad (21)$$

Using the data in Table 1 one obtains $U_c = 92 \text{ m/s}$. Note that Eq. (21) is not the long wavelength approximation obtained by setting $k = 0$ in Eq. (18). The latter gives $U_{cm} = \infty$ and $\omega = 0$.

By doubling the gap h one obtains the curve shown in Fig. 4, for which $U_{cm} = 184 \text{ m/s}$ and $f_c = 35 \text{ Hz}$. Similarly, by halving the stiffness K_s , one obtains the curve shown in Fig. 5, for which $U_{cm} = 119 \text{ m/s}$ and $f_c = 34 \text{ Hz}$. Finally, by halving

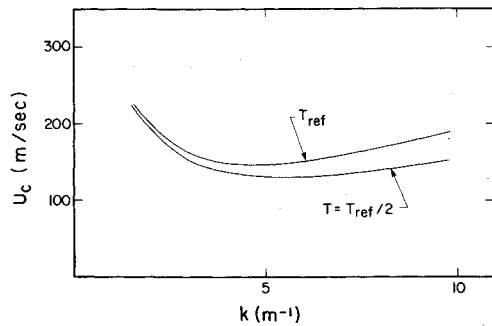


Fig. 6 Tension effect.

the tension T , one obtains the curve shown in Fig. 6, for which $U_{cm} = 130$ m/s and $f_c = 30$ Hz. Each of these trends is identical to the corresponding trend observed numerically in Ref. 1.

As mentioned above, the negative stiffness-positive stiffness argument outlined in Ref. 1 implies a static instability or divergence problem. The analysis presented here highlights the dynamic nature of the problem. For example, Eq. (15) shows that when U equals zero the angular frequency ω would be given by

$$\omega = \pm \sqrt{-C/A} \quad (22)$$

This implies that, as expected, waves due to a disturbance initiated at some value of x propagate both to the left and to the right in Fig. 2. But as U increases from zero, the speed of the left running waves decreases, and when $C=0$ they begin to be swept downstream. For a given k this occurs at a speed $U < U_c$. Hence, at the onset of instability, information propagates only downstream.

The major drawback of the present work is that it ignores end boundary conditions and variations along the trunk. One would expect this to cause significant error if the wavelength were of the order of some system characteristic dimension such as the trunk girth. However, here, even though the wavelength is typically 1.25 m, which is an appreciable fraction of the 3.5-m trunk girth, the errors appear to be small.

Acknowledgments

This work was inspired by the work of a UTIAS colleague, R. LeBlanc, on flow in lung airways. The work was partly funded by a Grant from the Natural Sciences and Engineering Research Council of Canada.

References

- ¹Boghani, A.B. and Fish, R.B., "Analysis of Trunk Flutter in an Air Cushion Landing System," AFFDL-TR-79-3102, Aug. 1979.
- ²Lamb, H., *Hydrodynamics*, Dover Publications, New York, 1932, Chap. IX, Article 232, pp. 373-375.
- ³Lighthill, M.J., *Waves in Fluids*, Cambridge University Press, Cambridge, 1978, Chap. 3.

From the AIAA Progress in Astronautics and Aeronautics Series . . .

TURBULENT COMBUSTION—v. 58

Edited by Lawrence A. Kennedy, State University of New York at Buffalo

Practical combustion systems are almost all based on turbulent combustion, as distinct from the more elementary processes (more academically appealing) of laminar or even stationary combustion. A practical combustor, whether employed in a power generating plant, in an automobile engine, in an aircraft jet engine, or whatever, requires a large and fast mass flow or throughput in order to meet useful specifications. The impetus for the study of turbulent combustion is therefore strong.

In spite of this, our understanding of turbulent combustion processes, that is, more specifically the interplay of fast oxidative chemical reactions, strong transport fluxes of heat and mass, and intense fluid-mechanical turbulence, is still incomplete. In the last few years, two strong forces have emerged that now compel research scientists to attack the subject of turbulent combustion anew. One is the development of novel instrumental techniques that permit rather precise nonintrusive measurement of reactant concentrations, turbulent velocity fluctuations, temperatures, etc., generally by optical means using laser beams. The other is the compelling demand to solve hitherto bypassed problems such as identifying the mechanisms responsible for the production of the minor compounds labeled pollutants and discovering ways to reduce such emissions.

This new climate of research in turbulent combustion and the availability of new results led to the Symposium from which this book is derived. Anyone interested in the modern science of combustion will find this book a rewarding source of information.

485 pp., 6 × 9, illus. \$20.00 Mem. \$35.00 List

TO ORDER WRITE: Publications Dept., AIAA, 1290 Avenue of the Americas, New York, N. Y. 10019